

## Finite element model for numerical analysis of strengthened reinforced concrete structures

## Modelo de elementos finitos para análise numérica de estruturas de concreto armado reforçadas



C. M. PALIGA <sup>a</sup>  
charlei.paliga@ufrgs.br

A. CAMPOS FILHO <sup>b</sup>  
americo@ufrgs.br

M. V. REAL <sup>c</sup>  
mauro@dmc.furg.br

### Abstract

The objective of this paper is to present a finite element model for the nonlinear analysis of reinforced concrete beams strengthened for flexure. The beams could be strengthened by the external bonding of steel plates or carbon fiber reinforced polymers (CFRP) to the beam tensile side. In the numerical simulation, the concrete was represented by bidimensional, eight nodes, isoparametric elements, according to a plane stress formulation. The steel reinforcement was represented by an embedded model. Each bar was considered as a more rigid line inside the concrete element, which resists only to axial efforts. The system of external reinforcement was represented by three nodes, quadratic, truss elements. The shear deformation in the adhesive layer causes a relative displacement between the external reinforcement and the concrete substrate. A six nodes, quadratic, unidimensional interface element was used for the evaluation of this slip and the corresponding bond stress. The model results were compared with experimental and numerical tests carried out by other authors. In the beams strengthened with steel plates, the maximum bond stress occurred in the zone of the plate curtailment, near to the supports. In the beams strengthened with CFRP, the maximum bond stress was initially observed in the region close to the flexural cracks. However, the maximum bond stress moved towards the supports, with the increase of the fiber sheet thickness.

**Keywords:** structural reinforcement, finite element method, reinforced concrete beams, carbon fiber reinforced polymers.

### Resumo

O objetivo deste trabalho é apresentar um modelo de elementos finitos para a análise não-linear de vigas de concreto armado reforçadas à flexão. O reforço pode ser feito através da colagem, na face tracionada da viga, ou de chapas de aço, ou de lâminas de polímeros reforçados com fibras de carbono (PRFC). Na simulação numérica, o concreto foi representado através de elementos isoparamétricos bidimensionais, de oito nós, para estado plano de tensão. A armadura foi representada através do modelo incorporado. Cada barra de armadura foi considerada como uma linha mais rígida dentro do elemento de concreto, que resiste apenas a esforços axiais. A discretização do sistema de reforço à flexão foi feita através de elementos de treliça plana, quadráticos, com três nós. A deformação por cisalhamento na camada de adesivo causa um deslocamento relativo entre o reforço e o substrato de concreto. Para o cálculo deste deslizamento, e das tensões de aderência, foi usado um elemento de interface unidimensional, de seis nós, com funções de interpolação quadráticas. O modelo foi testado através de resultados experimentais e numéricos realizados por outros autores. Para vigas reforçadas com chapas de aço, as maiores tensões de aderência ocorreram nas proximidades dos apoios. Nas vigas reforçadas com PRFC, as maiores tensões de aderência surgiram inicialmente na região das fissuras de flexão. Porém, com o aumento da rigidez do reforço, as máximas tensões de aderência deslocaram-se para os apoios.

**Palavras-chave:** reforço estrutural, método dos elementos finitos, vigas de concreto armado, compósitos de PRFC.

<sup>a</sup> Universidade Federal do Rio Grande do Sul, PPGEC, charlei.paliga@ufrgs.br, Av. Osvaldo Aranha, 99 - 3º andar, Porto Alegre, Brasil;

<sup>b</sup> Universidade Federal do Rio Grande do Sul, PPGEC, americo@ufrgs.br, Av. Osvaldo Aranha, 99 - 3º andar, Porto Alegre, Brasil;

<sup>c</sup> Fundação Universidade Federal do Rio Grande, CPGEO, mauro@dmc.furg.br, Av. Itália, km 8, Campus Carreiros, Rio Grande, Brasil;

## 1 Introduction

Although the reinforced concrete is a well known material of good performance and widespread use in the civil construction, its durability is a matter of high interest in the current days. The reinforced concrete structures are initially supposed to have a long life cycle. Nevertheless, design misconception, low quality materials and construction errors, allied to the lack of maintenance, have produced situations where structures have lost their functionality.

In this way, the economic development of a country challenges the civil construction industry regarding to the country infrastructure maintenance, i.e. the conservation of bridges, ports, airports, dams, public buildings, and so forth.

The first step in the process of structure maintenance is the assessment of its integrity and the investigation of the causes of its deterioration. The next step is the recovery of the initial conditions for which the structure was designed, which is called a repair design. Moreover, changes in the structure use may generate a situation where the structure load capacity must be increased. In this case, it is necessary a strengthening design.

Among the main techniques of structural repair and strengthening, there are the epoxy bonded steel plates and the application of composite materials, such as the external bonding of fiber reinforced polymer (FRP) sheets, to reinforced concrete beams and slabs.

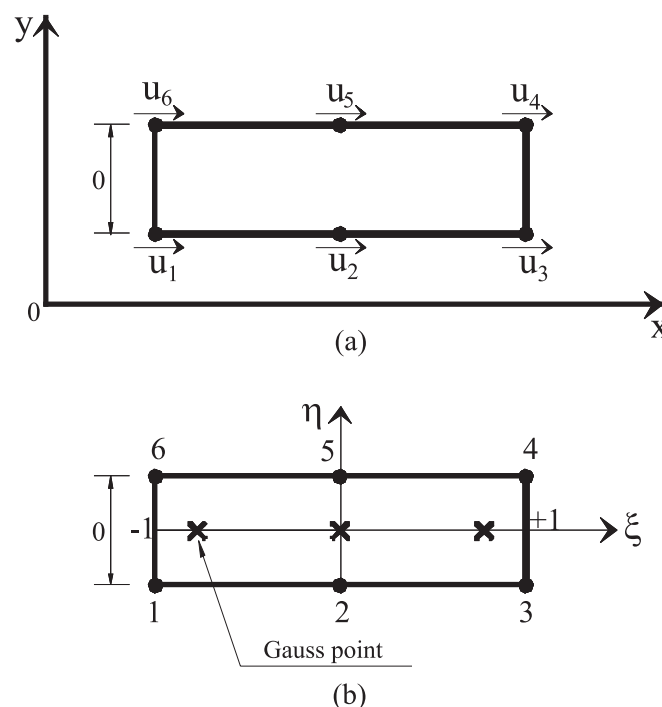
The first one has the advantages of economy and simplicity of execution. It permits the strengthening of the

structural element without a significant enlargement of its dimensions (Beber [1]). However, the high weight of the steel plates, which makes difficult its transportation and handling, and the possibility of corrosion after long periods of exposition to the atmosphere are some drawbacks of this technique. The second technique has as main advantages the high mechanical performance of the carbon fibers reinforced polymers (CFRP), its resistance to corrosion, and its low weight. However, the high cost of the composite materials has been limiting its use for a long time (Garcez et al. [2]).

There are many uncertainties about the behavior of structures strengthened for flexure. One of the principal motivations of this study is to analyze the change from the ductile failure mode to the brittle failure mode by debonding of the strengthening system. The researches about numerical models for strengthened structures are justified because it is necessary to predict its behavior under service loads as well as to preview the increase of its load carrying capacity. Among the works already developed on this matter it may be mentioned the ones by Ziraba and Baluch [3], Ascione and Feo [4], and by Adhikary e Mut-suyoshi [5].

The objective of this work is to present a finite element model for the nonlinear analysis of reinforced concrete beams strengthened for flexure to predict both its behavior under service loads and its failure mode. The most observed failure mode of reinforced concrete beams strengthened for flexure is the adherence failure between the externally

Figure 1 – Interface element: global reference system (a) and local reference system (b)



bonded reinforcement and the concrete (Thomsen [6]). Thus, a special interface element was introduced in the model to simulate the bond between the two materials, which permits the evaluation of the bond stresses.

The finite element model developed in this work enables to trace the structural response of reinforced concrete beams strengthened for flexure from the initial loading up to the failure. With the interface element, the bond stress distribution between the external reinforcement and the concrete substrate can be obtained along the whole extension of the strengthening system. Once the bond stress distribution is known, the model can predict the premature beam failure caused by the external reinforcement debonding.

## 2 Finite element method formulation

The initial step of the finite element method is to divide the midplane structure into little surface elements (called finite elements), which are connected to each other by nodal points. In the displacement solution, the problem unknowns are the nodal point displacements. The strains inside the element are calculated from the nodal displacements. The stresses are evaluated through the strains using a constitutive stress-strain law. Finally, the nodal equilibrium between external loads and internal forces is obtained through an incremental-iterative process.

### 2.1 Element for the concrete

In this work, plane stress elements are used to represent the concrete. These elements are bidimensional, isoparametric, quadratic, with eight nodal points. Each node has two degrees of freedom, i.e. the translations in the "x" and "y" directions of the global reference system.

### 2.2 Reinforcement modelling

The embedded model proposed by Elwi e Hruday [7] is used in this work to represent the steel reinforcement. In this formulation, it is supposed that there is perfect adherence between the steel rebar and the concrete that encloses it. In this way, the displacement at any point in the reinforcement element is obtained by the interpolation of the concrete element nodal displacements. It is

considered that a rebar resists only to axial efforts in its longitudinal direction.

One of the main advantages of this model is that the rebar may have an arbitrary disposition inside the concrete element. This can be made without the creation of additional unknowns in the problem.

When the embedded model is used, the steel reinforcement stiffness matrix has the same dimensions of the concrete stiffness matrix. The reinforced concrete stiffness matrix is the sum of these two matrices.

### 2.3 Element for the strengthening system

The strengthening system is modeled through the use of plane truss bar elements. These elements are quadratic, with three nodal points. These elements resist only to axial efforts in the longitudinal direction.

### 2.4 Interface element between the concrete and the strengthening system

The efforts transmission between the concrete and the strengthening system produces shear stresses in the interface between the two materials. The relative displacements between the two materials should be known to permit the evaluation of these shear stresses. This is possible due to the introduction of a special interface element to simulate the adherence between the concrete and the strengthening system. This interface element is based on the work of Adhikary and Mutsuyoshi [5].

This one-dimensional interface element is isoparametric, with six nodal points, quadratic shape functions and it has zero thickness, as it is presented in Figure 1.

Because the interface element thickness is zero, it is sufficient to represent it through the equivalent pseudo nodes 1', 2' and 3', as it is shown in Figure 2. Thus, the element definition is made through the "x" coordinate of the pseudo nodes, in the structure global system.

In the finite element discretization process, the top face nodes of the interface element will be coincident with the nodes of the adjacent concrete element. The nodes of the bottom face of the interface element will coincide to the nodes of the adjacent strengthening element. In the Figure 3, it is illustrated how the adjacent strengthening and concrete elements are connected by the interface element.

Usually, the stresses are functions of the strains. But in the case of the bond stresses between the concrete and the strengthening system, the shear stresses are functions of the relative displacements between these two materials. The displacement at any point of the interface element is obtained through the interpolation of the element nodal displacements. Thus, the relative displacement at any point of the interface element can be evaluated by the use of the following expression:

$$s = N'_1(u_6 - u_1) + N'_2(u_5 - u_2) + N'_3(u_4 - u_3) \quad \text{Equation 1}$$

Figure 2 – Equivalent pseudo nodes

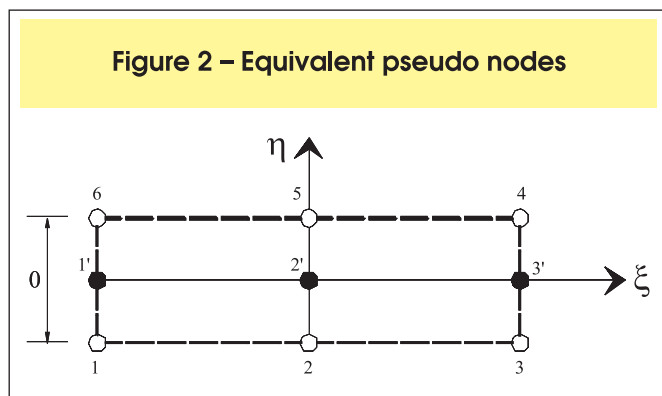
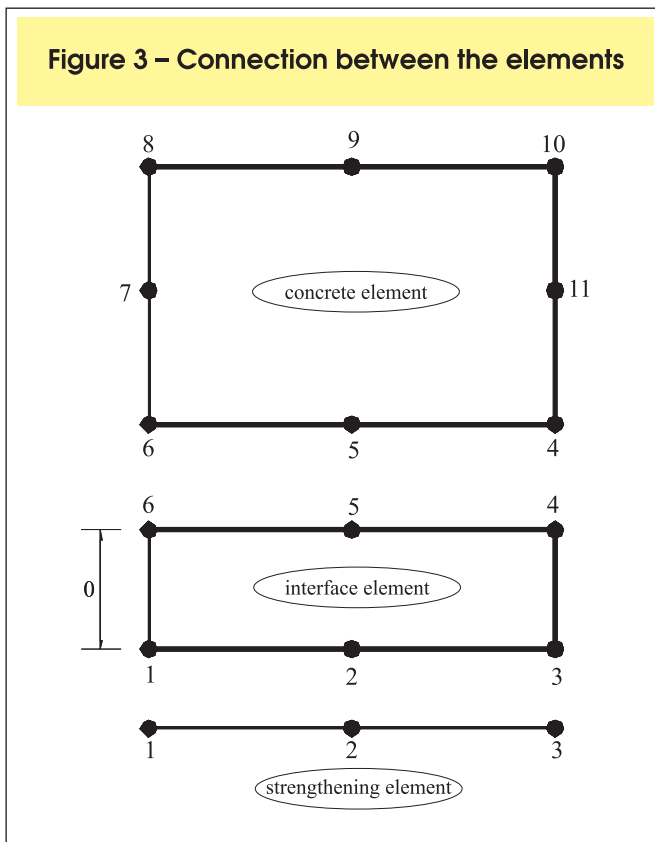


Figure 3 – Connection between the elements



### 3 Material constitutive models

The consistent simulation of the material mechanical behavior is very important for a successful structural analysis through the finite element method. Thus, mathematical models must be established for the constitutive relations (stress-strain laws) of the concrete, the steel, and the strengthening system.

For the strengthening system, two constitutive laws must be defined. A stress-strain law must be established for the resistant part (composite material or the steel plate). A stress-slip law must be prescribed to the part responsible for the transmission of the stresses between the concrete and the composite material or steel plate (adhesive).

These constitutive relations must represent the real mechanical behavior of the material when submitted to the strains and stresses due to the loading imposed on the structure.

#### 3.1 Concrete

A bidimensional constitutive model, developed by Darwin e Pecknold [8], is employed to represent the concrete behavior under short term monotonic loads. This model is appropriated to the nonlinear analysis of structures by the finite element method, and it is recommended by the CEB-FIP Model Code 1990 [9].

At first, the main directions and the strain components are determined. Then, the concept of equivalent uniaxi-

al strain and the bidimensional failure criterion of Kupfer and Gerstle [10] are used to evaluate the secant elasticity moduli in the principal strain axes. With the secant elasticity moduli, which are functions of the strain state at the point, the total stresses in the principal strain directions are calculated by using an orthotropic constitutive law.

The concrete cracking is represented by the smeared crack approach. This model has the advantage that it is not necessary to redefine the finite element mesh for each new crack that appears in the structure. It is only necessary to prescribe an additional constitutive equation for the concrete in the cracked state.

In this way, after the concrete cracking strain is reached, the concrete between cracks contribution to the tensile stresses resistance (tension stiffening) is represented by a linear descending branch in the stress-strain relation for the tensioned concrete.

It is also considered that a certain amount of shear effort is transmitted through the crack plane via the mechanisms of aggregate interlock and the dowel effect of the rebars that cross the crack plane. A reduced shear modulus is introduced in the model to include this effect.

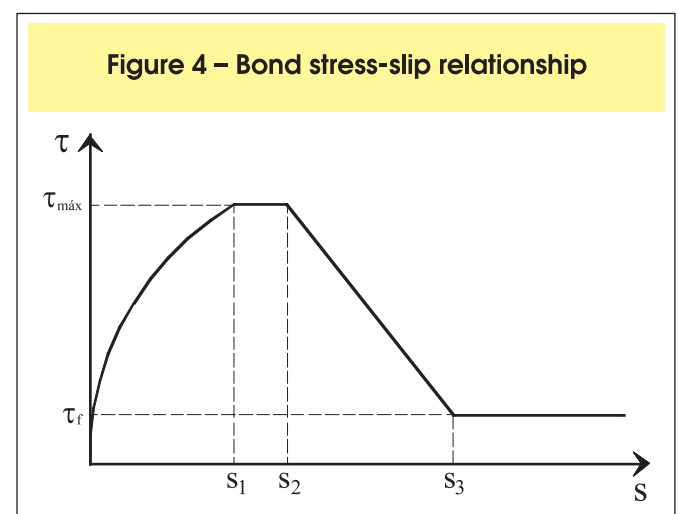
If the concrete compression strength under a biaxial stress state (biaxial compression or tension-compression) is reached at some point, this point is considered as crushed. A crushed point can support an increasing of the strain only if it is accompanied by a decreasing compression stress. Thus, after the concrete crushing, a descending line is adopted for the constitutive equation of the compressed concrete.

The constitutive equation in the main strain axes is selected according to the concrete state: intact, cracked or crushed. Then, the constitutive relation in the global reference system of the structure is obtained by a rotation transformation.

#### 3.2 Steel reinforcement

The reinforcement embedded model considers that each rebar resists only to normal forces in the axis tangent di-

Figure 4 – Bond stress-slip relationship



rection. Thus, it is only necessary a uniaxial constitutive relation to model the steel behavior.

In this way, the steel is modeled according to an elastic bilinear approach. After the yielding strain is reached, a strain hardening is considered until the material failure.

For the sake of simplicity, the material behavior in compression is simulated in the same way as in tension.

### 3.3 Strengthening system

The behavior of the carbon fiber reinforced polymers (CFRP) is linear elastic until the ultimate elongation is reached, and then a brittle failure occurs. When the strengthening is made by the bonding of steel plates, it is considered that this material has an elastic perfectly plastic behavior.

### 3.4 Interface between the concrete and the strengthening system

The model for the adherence between the concrete substrate and the strengthening system obeys the bond stress-slip relationship proposed in the CEB-FIP Model Code 1990 [9], as it is shown in Figure 4. Therefore, the bond stress “ $\tau$ ” between the concrete substrate and the external reinforcement can be evaluated as a function of the slip “ $s$ ”, according to the model presented in Figure 4, and using the following equations 2, 3, 4 and 5.

The necessary parameters for the calculation of the bond stress when the strengthening is made by using steel plates were extracted from the CEB-FIP Model Code 1990 [9], for the case of bond stress between the concrete and smooth reinforcement bars. The values of these parameters are shown in Table 1.

The parameters adopted for the evaluation of the bond stress between the concrete and the strengthening composite material were obtained from the studies made by Silva [11] and can be found in Table 2.

## 4 Finite element model results and discussion

An efficient finite element model for the nonlinear analysis of reinforced concrete beams strengthened for flexure

$$\tau = \tau_{\text{máx}} \left( \frac{s}{s_1} \right)^\alpha, \text{ for } 0 \leq s \leq s_1 \quad \text{Equation 2}$$

$$\tau = \tau_{\text{máx}}, \text{ for } s_1 < s \leq s_2 \quad \text{Equation 3}$$

$$\tau = \tau_{\text{máx}} - (\tau_{\text{máx}} - \tau_f) \left( \frac{s - s_2}{s_3 - s_2} \right), \text{ for } s_2 < s \leq s_3 \quad \text{Equation 4}$$

$$\tau = \tau_f, \text{ for } s > s_3 \quad \text{Equation 5}$$

must be able to predict the overall structure response, including the different failure modes.

To confirm the numerical model efficiency, were simulated a several cases of reinforced concrete beams strengthened for flexure with CFRP or steel plates. Some results obtained in the analyses, which prove the validity of the model, are presented here. These beams were experimentally or numerically tested by other authors and their results were published in the literature.

### 4.1 Beam simulated by Ascione and Feo (4)

This beam was tested by Jones et al. [12] and it was used by Ascione and Feo [4] to validate their numerical model. It was a simply supported beam with a cross section of 15.5 x 22.5 cm<sup>2</sup> and 230 cm long. This beam was reinforced with a steel plate bonded to the bottom face. The steel plate had a cross section of 12.5 x 0.6 cm<sup>2</sup> and was 220 cm long. The beam was loaded by two concentrated

**Table 1 – Parameters for defining the bond stress-slip relationship of steel plates (9)**

	Cold drawn wire		Hot rolled bars	
	Good bond conditions	All other bond conditions	Good bond conditions	All other bond conditions
$s_1 = s_2 = s_3$	0.01 mm	0.01 mm	0.1 mm	0.1 mm
$\alpha$	0.5	0.5	0.5	0.5
$\tau_{\text{máx}} = \tau_f$	$0.1 \sqrt{f_{ck}}$	$0.05 \sqrt{f_{ck}}$	$0.3 \sqrt{f_{ck}}$	$0.15 \sqrt{f_{ck}}$

**Table 2 – Parameters for defining the bond stress-slip relationship of the CFRP laminate (11)**

CFRP	
$s_1$	0.08 mm
$s_2$	0.08 mm
$s_3$	0.65 mm
$\alpha$	0.6
$\tau_{m\acute{o}x}$	3.5 MPa
$\tau_f$	0.1 $\tau_{m\acute{o}x}$

forces applied at a distance of one third of the span from the supports. The tension reinforcement consisted of two 20 mm diameter steel reinforcing bars. The compression reinforcement was composed of two 6 mm diameter steel reinforcing bars. To avoid a brittle shear failure, it was used a transversal reinforcement formed by 6 mm diameter stirrups with a uniform spacing of 7.5 cm.

The reinforced concrete beam strengthened for flexure tested experimentally by Jones et al. [12] and numerically simulated by Ascione and Feo [4] is presented in Figure 5. Due to symmetry of geometry and loading pattern only one-half of the beam was analyzed. A mesh of eight elements along the length and two elements along the height was used to represent the concrete. Seven elements were used to model the strengthening system and its interface with the concrete, as shown in Figure 6. The material properties of the problem are shown in Table 3.

The bond stress distribution along the interface between the steel plate and the concrete is presented in Figures 7, 8 and 9. Figure 7 corresponds to a load level of 60 kN, which is equal to 33% of the experimental failure load.

Figure 8 corresponds to 77% of the experimental collapse load, whereas Figure 9 corresponds to a load very close to the beam failure.

According to Jones et. al [12], the failure occurred suddenly by debonding of the steel plate from the concrete substrate under a load  $P$  of 182 kN. A load increment of 1 kN was employed in the numerical analysis. In each load step, an iterative process is used until the structure reaches equilibrium or the failure occurs. For a load  $P$  of 178.25 kN, it was not possible to reach an equilibrium state and so the structure collapsed. The difference between the numerical failure load to the experimental failure load was of -2.06%.

The Figure 10 permits to compare the numerical model results with the data from the experimental test, for the strains along the length of the steel plate, for three loading levels (33%, 77% and near to the failure).

#### 4.2 Beams tested by Beber (13)

Beber [13] performed an experimental investigation about reinforced concrete beams strengthened for flexure with carbon fiber sheets. The beams reinforced with one layer of CFRP sheet, with cross-sectional area equals to 0.1332 cm<sup>2</sup>, were called VR3 and VR4. The beams strengthened with ten layers of CFRP sheet, with total cross-sectional area equals to 1.332 cm<sup>2</sup>, were named VR9 and VR10.

The beams had a cross section of 12 x 25 cm<sup>2</sup> and were 250 cm long. The tension reinforcement was composed of two 10 mm diameter, grade CA-50, steel reinforcing bars, which corresponds to a reinforcement rate  $\rho=0.58\%$ . This low reinforcement rate permitted the assessment of the beams strengthening performance without reaching a brittle failure due to concrete crushing (Beber [13]). The compression reinforcement consisted of two 6 mm diameter, grade CA-60, steel reinforcing bars. The shear rein-

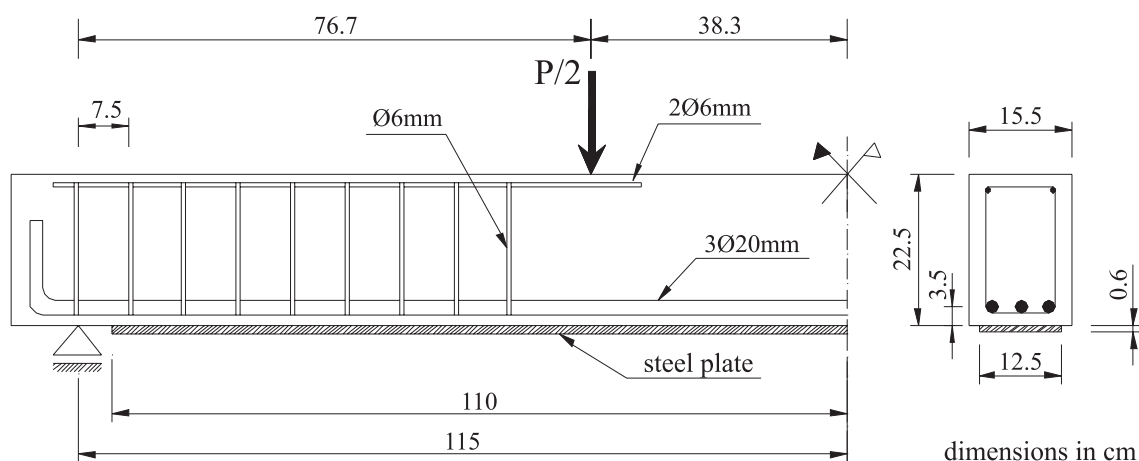
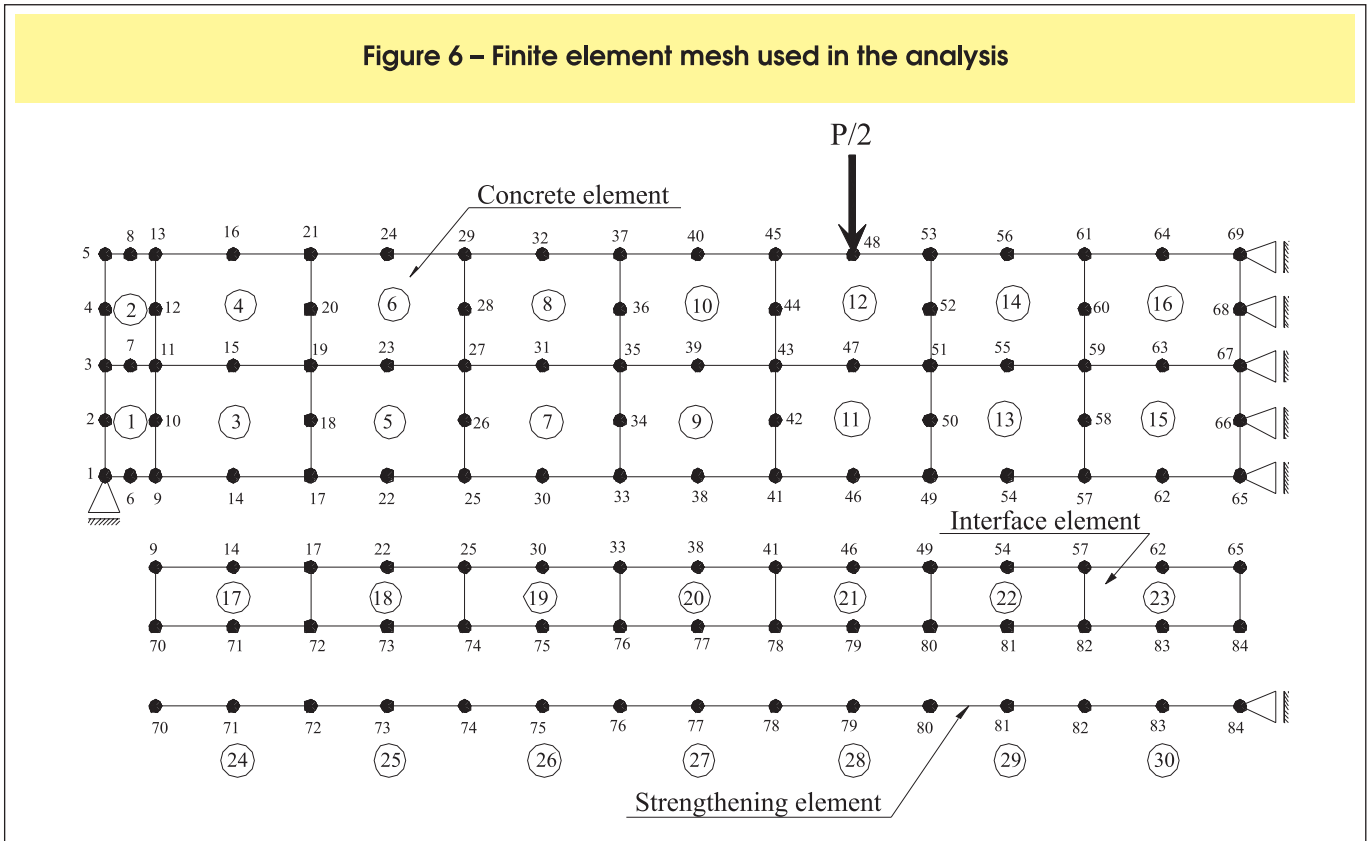
**Figure 5 – Reinforced concrete beam strengthened with steel plate**


Figure 6 – Finite element mesh used in the analysis



forcement consisted of 6 mm diameter, grade CA-60, steel stirrups with a uniform spacing of 11 cm, along the whole beam length. The tested beams detailing and the loading pattern can be observed in Figure 11.

The mechanical properties of the materials: concrete, steel rebars and CFRP sheet are summarized in Table 4. The finite element mesh used in the numerical analysis of the beams tested by Beber [13], observed the proportions of each example, has the same aspect of that shown in Figure 6, which was used in the simulation of the beam of Ascione and Feo [4].

The numerical load-deflection curve is compared to the experimental curve for beams VR3 and VR4, in Figure 12.

The failure load predicted by the proposed model was 65.25 kN. The experimental failure load for beam VR3 was 65.2 kN, whereas beam VR4 collapsed for a load of 62 kN.

In Figure 13, a comparison is made between the numerical and experimental results for the fiber maximum strain, as the loading is increased, for the beams strengthened with one layer of CFRP sheet.

The bond stress distribution obtained numerically, for different loading levels, is shown in Figure 14. According to Beber [13], the failure of the beams strengthened with one layer of CFRP sheet was caused by excessive plastic strain of the tension reinforcement and there was no external reinforcement debonding. In Figure 14, it can be observed

Table 3 – Beam simulated by Ascione and Feo (4) – Material properties

Concrete	Tension reinforcement $\phi$ 20mm	Compression reinforcement and stirrups $\phi$ 6mm	Steel plate
$f_{cm} = 30$ MPa	$f_y = 430$ MPa	$f_y = 324$ MPa	$f_y = 246$ MPa
$f_{ctm} = 2.91$ MPa	$E_s = 200$ GPa	$E_s = 200$ GPa	$E_s = 200$ GPa
$E_{co} = 31$ GPa	-	-	-
Interface	$k_s = 50$ MPa/mm	$\tau_{max} = 5$ MPa	-

**Figure 7 – Bond stress distribution between the concrete and the steel plate: P = 60 kN**

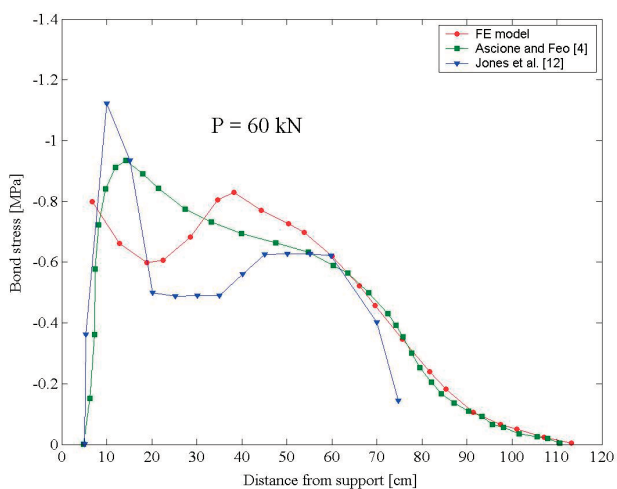


**Figure 8 – Bond stress distribution between the concrete and the steel plate: P = 140 kN**

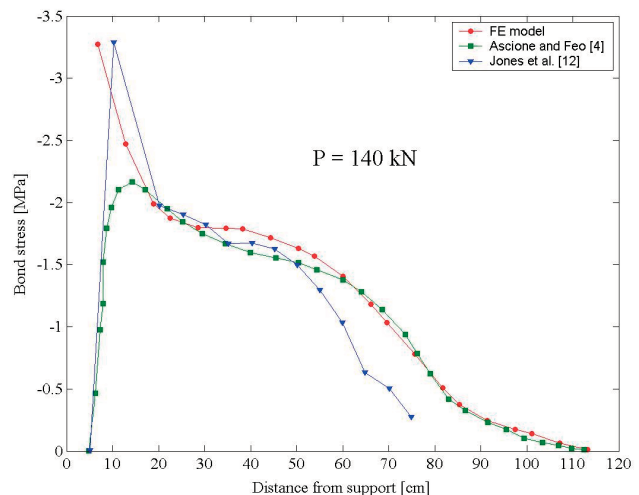


**Figure 9 – Bond stress distribution between the concrete and the steel plate: near to the failure**

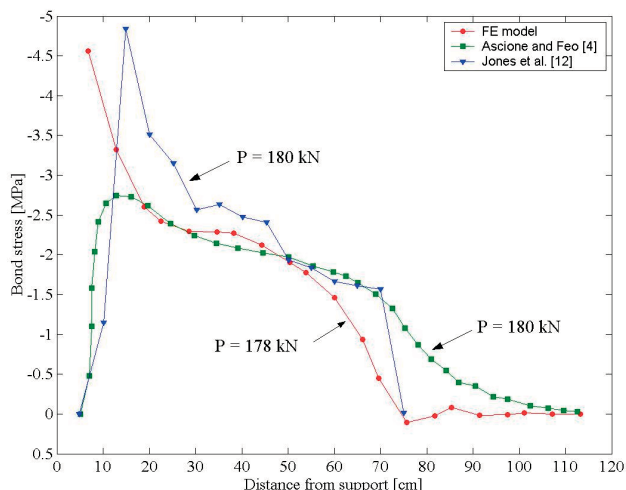
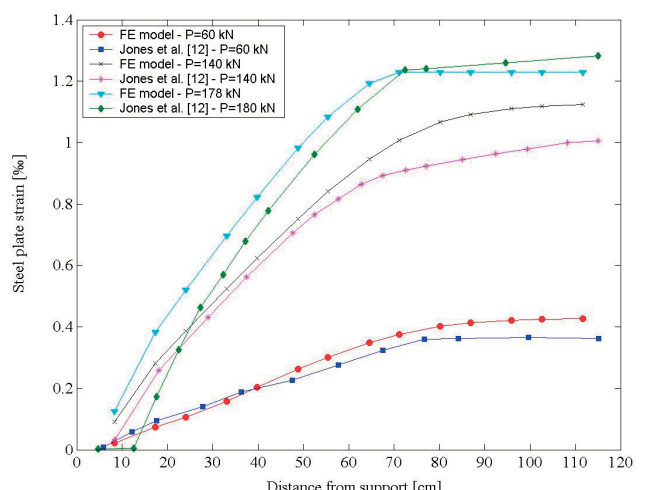


**Figure 10 – Strains along the steel plate**



that the bond stresses did not reach the ultimate bond stress shown in Table 4. Therefore, the model predicted accurately the failure mode observed in the tests.

The diagram of Figure 15 permits to assess the interaction among the normal stress in fiber, the normal stress in the steel reinforcement and the bond stress in the interface between the fiber and the concrete. The stresses are normalized in relation to the corresponding maximum value. These stress distributions were obtained at the last load step in which equilibrium convergence was achieved, preceding the beam failure (P=65 kN).

The assessment of the diagrams in Figure 15 permits to determinate, easily, that the normal stress in the fiber increases from its extremity to midspan. Another important aspect is associated with the peak of the bond stress curve. The maximum value is due to the sudden increase of the tension stress in the fiber, in the region of the concentrated load. This fact is a consequence of the concrete cracked state and the tension reinforce-

ment yielding in this region. These phenomena cause an increasing stress variation in the fiber, and bond stresses must appear to satisfy the equilibrium conditions.

According to what is reported by Beber [13], the beams strengthened with ten layers of CFRP sheet (VR9 and VR10) showed a failure mode related to the debonding of the fiber sheets close to the supports. The failure load of the beam VR9 was 129.6 kN. The beam VR10 collapsed for a load of 137 kN. The finite element model predicted a failure load of 131.75 kN.

The experimental and numerical load versus midspan deflection curves for the beams strengthened with ten layers of CFRP sheet can be compared in Figure 16. In Figure 17, it is shown the evolution of the fiber maximum strain with the increasing load.

The bond stress distributions numerically obtained for various loading levels, are shown in Figure 18. The interaction among the normal stress in the fiber, the normal stress in the steel reinforcement and the bond stress, for a load level equals to 131.5 kN and normal-

Figure 11 – Detailing of the beams tested by Beber (13)

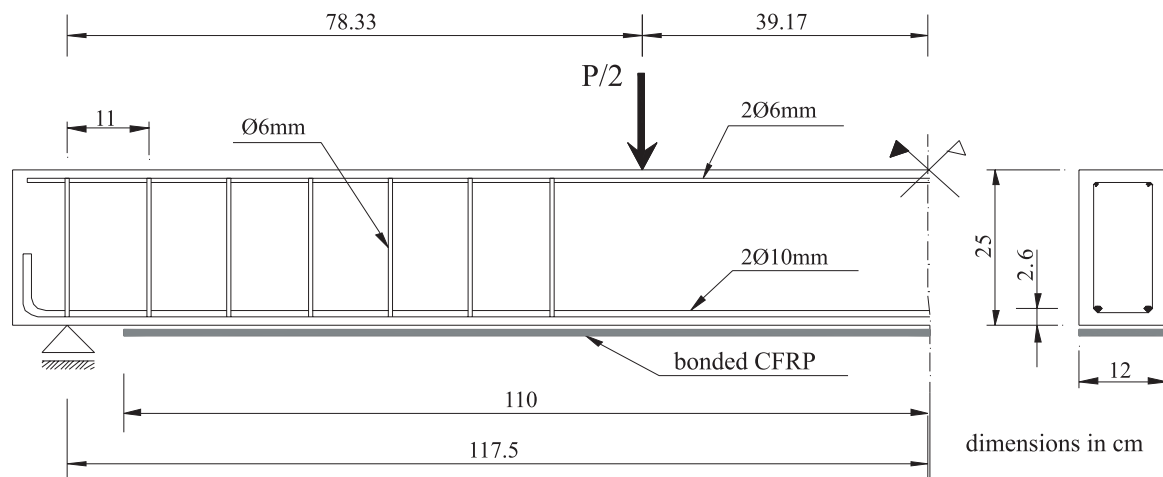
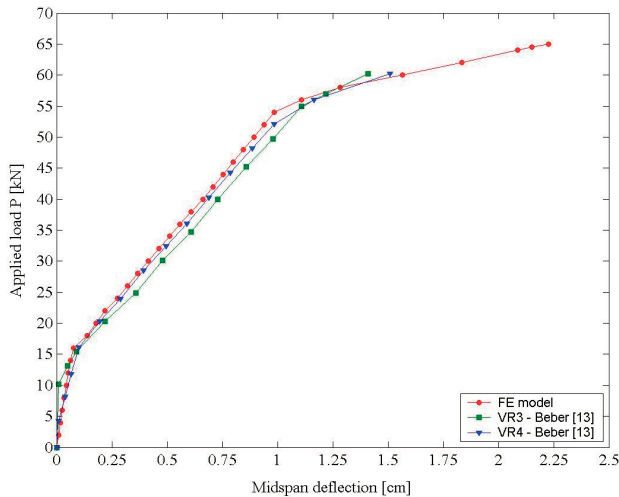


Figure 12 – BeamsVR3 and VR4: load versus midspan displacement curves



ized in relation to the corresponding maximum value, is indicated in Figure 19. In this way, can be observed a tendency of the behavior of the beams strengthened with ten layers of CFRP.

The brittle failure mode of the beams VR9 and VR10

is related to the ductility reduction caused by the strengthening system application. The cross section discontinuity near the supports, changing from a reinforced concrete cross section to a CFRP strengthened cross section, can cause a stress concentration in this region. Moreover, the stress transference between the CFRP sheet and the concrete can induce the fiber debonding from its extremity (Thomsen [6]). This fact was experimentally observed and it was accurately predicted by the numerical model.

The bond stress increasing, in the region of the concentrated load (Figure 19), is due to the yielding of the tension reinforcement. In the zone wherein the reinforcement has not yielded, the tension efforts are distributed between the steel reinforcement and the fiber sheets. However, inside the zone where the steel reinforcement has yielded, the fiber has to resist a larger portion of the tension efforts. Therefore, in the transition length from one zone to another, there is a high stress gradient in the fiber. The bond stress value depends on the variation of the normal stress in the externally bonded reinforcement, so the bond stress has a significant increasing in this transition length. Nevertheless, the bond stress values are almost reduced to zero in the beam central region (Figure 19), because there are no more variations in the fiber tension stress.

Table 4 – Beams tested by Beber (13) – Material properties

Concrete	Tension reinforcement $\phi$ 10mm	Compression reinforcement and stirrups $\phi$ 6mm	CFRP laminate
$f_{cm} = 33.58$ MPa	$f_{ym} = 565$ MPa	$f_{ym} = 738$ MPa	$\sigma_{rup} = 3,400$ MPa
$f_{ctm} = 3.14$ MPa	$E_s = 210$ GPa	$E_s = 210$ GPa	$E_R = 230$ GPa
$E_{co} = 32,196$ GPa	-	-	-
Interface	$k_s = 43.75$ MPa/mm	$\tau_{max} = 3.5$ MPa	-

**Figure 13 – Beams VR3 and Vr4: maximum strain in the CFRP**

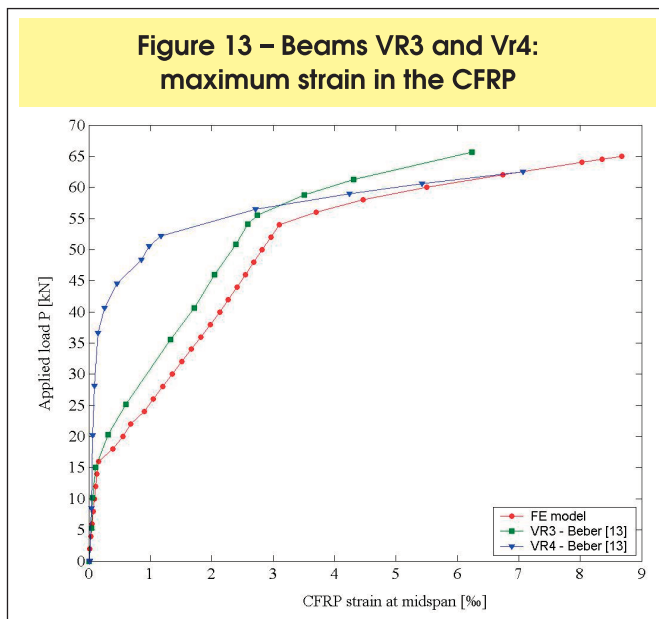


**Figure 14 – Beam strengthened with one layer of CFRP sheet: bond stress distribution**

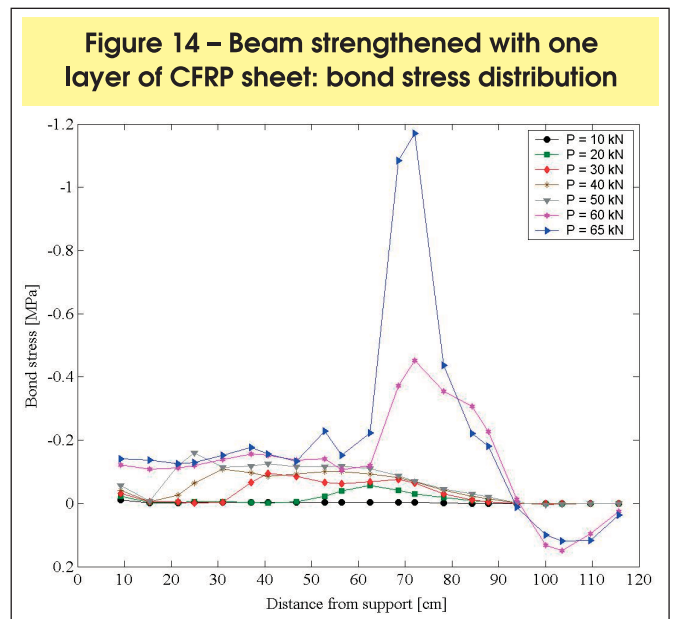


**Figure 15 – Beam strengthened with one layer of CFRP sheet: normalized stresses diagram**

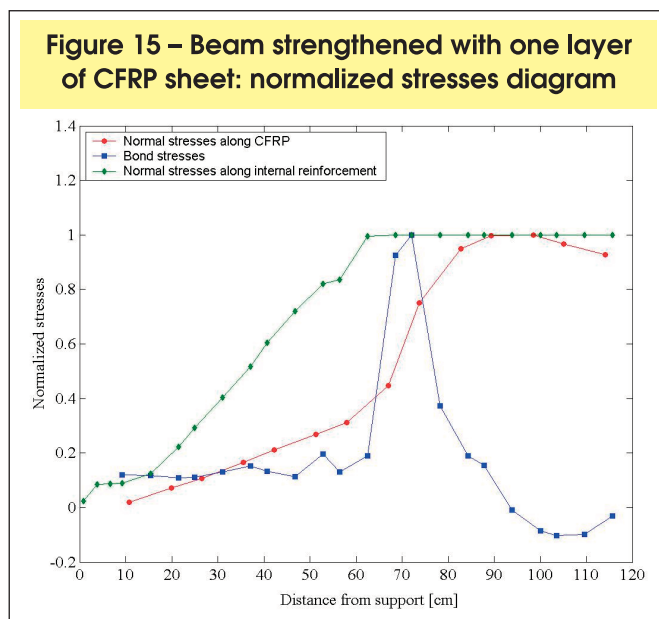
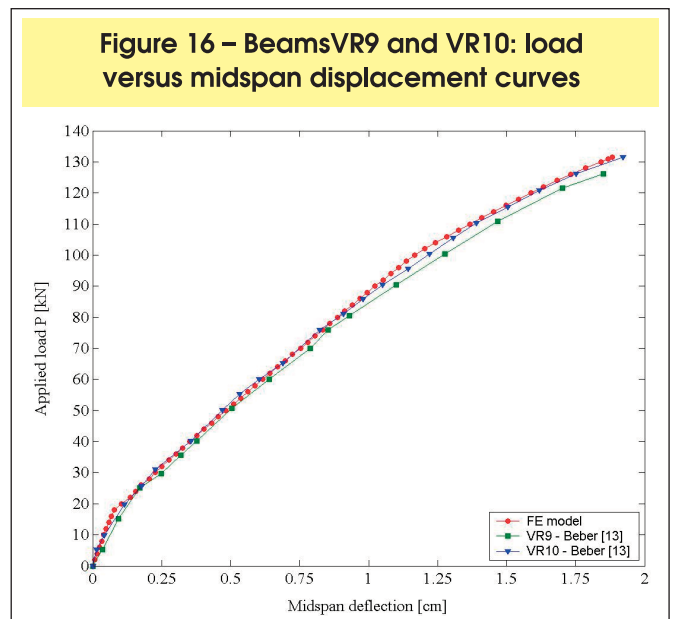


**Figure 16 – Beams VR9 and VR10: load versus midspan displacement curves**



## 5 Conclusions

The two main objectives of this work were: to present a finite element model for the nonlinear analysis of reinforced concrete beams strengthened for flexure; and to show the importance of the consideration of the bond-slip effect between the strengthening system and the reinforced concrete beam.

The results of the proposed finite element model have shown a good agreement in stiffness, strength and failure mode with the experimental and numerical results obtained by other authors. Therefore, these results validate the finite element model developed in this paper.

The analysis of the model results shows that the maximum bond stress value can be obtained in different positions along the length of the strengthening system. For the steel plate strengthening system, the debonding of the plate initiated in the plate curtailment near to the beam support. For the CFRP sheet strengthening system, it was observed that the increasing of the fiber cross-sectional area moves the maximum bond stress from the zone of the concentrated load towards the extremity of the fiber sheet close to the beam support (Figures 14 and 18).

## 6 Acknowledgments

This study was supported by the Brazilian National Council

**Figure 17 – Beams VR9 and Vr10: maximum strain in the CFRP**

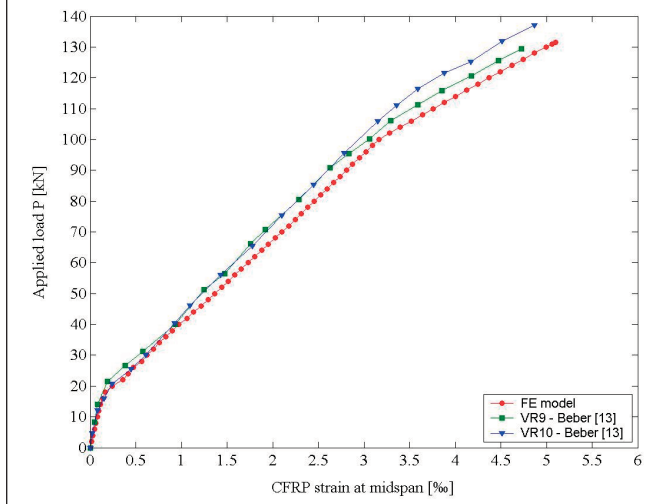
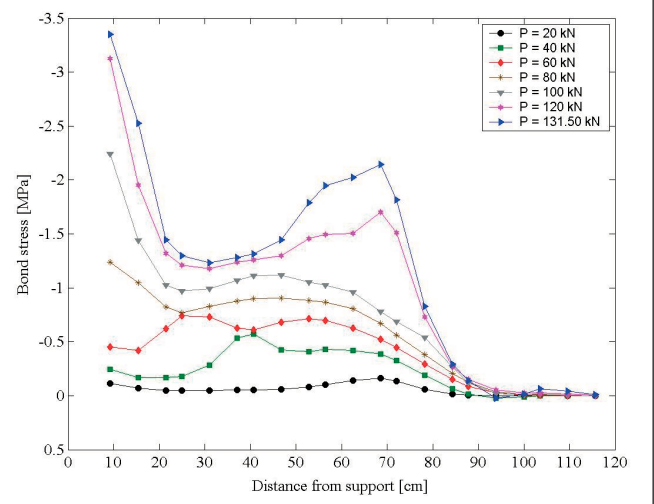


**Figure 18 – Beam strengthened with ten layers of CFRP sheet: bond stress distribution**

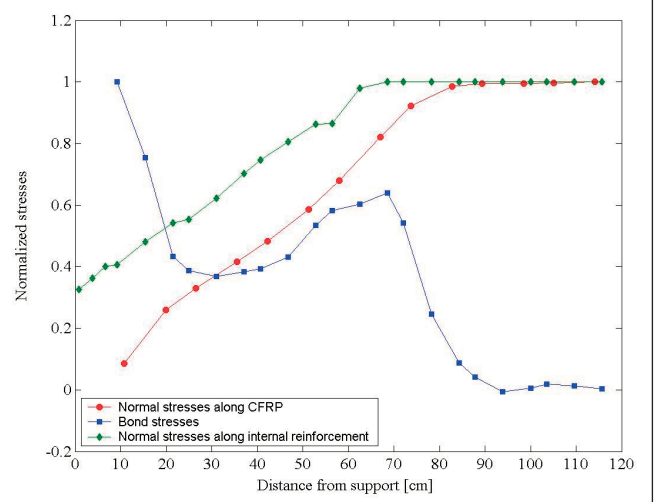


for Scientific and Technological Development (CNPq). This support is gratefully acknowledged by the authors.

## 7 References

- [01] BEBER, A. J. Comportamento estrutural de vigas de concreto armado reforçadas com compósitos de fibra de carbono, Porto Alegre, 2003, Tese (doutorado) – Programa de Pós-Graduação em Engenharia Civil, Universidade Federal do Rio Grande do Sul, 317 p.
- [02] GARCEZ, M. R.; MENEGHETTI, L. C.; CAETANO, L. F.; CAMPAGNOLO, J. L.; SILVA FILHO, L. C. P. Utilização de fibras de alto desempenho como reforço a flexão em vigas de concreto armado. In: Congresso Latinoamericano de Patologia de La Construcción, 8º, Asunción, 2005, Anais, Paraguay, 2005, v.2, p.65-72.
- [03] ZIRABA, Y. N.; BALUCH, M. H. Computational Model for reinforced concrete beams strengthened by epoxy steel plates. *Finite Elements in Analysis and Design*, v.20, p.253-271, 1995.
- [04] ASCIONE, L.; FEO, L. Modeling of composite/concrete interface of RC beams strengthened with composite laminates. *Composites: Part B*, v.31, p.535-540, 2000.
- [05] ADHIKARY, B. B.; MUTSUYOSHI, H. Numerical simulation of steel-plate strengthened concrete beam by a non-linear finite element method model. *Construction and Building Materials*, v.16, p.291-301, 2002.
- [06] THOMSEN, H.; SPACONE, E.; LIMKATANYU, S.; CAMATA, G. Failure mode analyses of reinforced concrete beams strengthened in

**Figure 19 – Beam strengthened with ten layers of CFRP sheet: normalized stresses diagram**



- flexure with externally bonded fiber-reinforced polymers. *Journal of composites for construction*, ASCE, v.8, n.2, 2004; p.123-131.
- [07] ELWI, A. E.; HRUDEY, T. M. Finite element model for curved embedded reinforcement. *Journal of Engineering Mechanics Division*, v.115, 1989; p.740-745.
- [08] DARWIN, D.; PECKNOLD, D. A. Nonlinear biaxial stress-strain law for concrete. *Journal of Engineering Mechanics Division*, v.103, 1977; p.229-241.
- [09] COMITÉ EURO-INTERNATIONAL DU BETON. CEB-FIP model code 1990; design code, London: Thomas Telford Services, 1993, 437 p.

- [10] KUPFER, H. B.; GERSTLE, K. H. Behavior of concrete under biaxial stresses. *Journal of Engineering Mechanics*, v.99, 1973; p.853-866.
- [11] SILVA, P.A.S.C.M. Modelação e análise de estruturas de betão reforçadas com FRP, Porto, 1999, Dissertação (mestrado) - Faculdade de Engenharia da Universidade do Porto, 254 p.
- [12] JONES, R.; SWAMY, R. N.; CHARIF, A. Plate separation and anchorage of reinforced concrete beams strengthened by epoxy-bonded steel plates. *The Structural Engineer*, v.66, n.5, 1988; p.85-94.
- [13] BEBER, A. J. Avaliação do desempenho de vigas de concreto armado reforçadas com lâminas de fibra de carbono, Porto Alegre, 1999, Dissertação (mestrado) - Programa de Pós-Graduação em Engenharia Civil, Universidade Federal do Rio Grande do Sul, 108p.